High-energy optical-absorption bands of transition-metal ions in fluoride host crystals*

Joseph F. Sabatini, Arthur E. Salwin, and Donald S. McClure
Department of Chemistry, Princeton University, Princeton, New Jersey 08540
(Received 2 December 1974)

Absorption bands in the region from 40 000 to 80 000 cm^{-1} have been found for the divalent ions of V, Cr, Mn, Fe, Co, and Ni in the host crystals $KMgF_3$, CaF_2, and MgF_2. Their spectral positions are near those of the free-ion $3d \rightarrow 4s$ transitions when corrected for crystal-field shifts. The f numbers are near 10^{-3} and most of the bands have a temperature-dependent absorption strength consistent with a vibronic absorption mechanism. It is concluded that these are well described as $3d \rightarrow 4s$ transitions.

I. INTRODUCTION

The optical spectra of transition-metal ions as impurities in ionic crystals have been vigorously investigated within the past two decades. The low-energy electronic transitions correspond to excitations within the transition-metal d orbitals, and it is upon these excitations that most studies have concentrated. Absorption bands of higher energy and higher intensity which cannot be assigned to intra-d-shell transitions are often called charge-transfer bands, but there has been little systematic study of these bands. An important contribution in this area, however, is the work of Tippins,[1] a systematic study of the high-energy spectra of the trivalent transition-metal ions in Al_2O_3.

Tippins showed that the strong absorption bands from about 4 to 8 eV correspond to a process in which the impurity metal ion acts as an acceptor of electrons from its near oxygen neighbors, or valence band of the Al_2O_3 crystal. A classical charge-transfer model correlated with the data fairly well. The bands show no structure, so the fine details of the charge-transfer process could not be uncovered.

Much more information about charge-transfer transitions has been collected from the spectra of liquid and glassy solutions and crystals of the heavier halogens. Jorgensen has reviewed this work up to 1970,[2] and more recent work is that of Day.[3] In these more moleculelike systems, the detailed expectations of molecular orbital theory[4] can be tested against the relatively sharp spectra observed. These results are giving reliable information about molecular orbital energy level ordering, spin-orbit contributions of ligand and metal, and other details of the excited states involved. Schatz and co-workers have obtained sharp spectra of $5d$ transition metals in octahedral halide environments and have used magnetic circular dichroism (MCD) to confirm assignments.[5-8] In the case of MgO: V^{++}, Modine has used MCD to confirm the identity of an oxygen-metal charge-transfer band.[9]

In all of the above studies, the metal ion has been found to act as an electron acceptor in these transitions. A possible exception may occur in the NaCl lattice doped with the divalent transition ions,[10] in which case the weaker transitions were assigned as $3d \rightarrow 4s$. Similar transitions have been seen in the pure oxides and chlorides.[11,12]

In this paper we present the results of a study[13,14] of the high-energy absorption bands of divalent transition-metal ions in the fluoride host crystals CaF_2, MgF_2, and $KMgF_3$. We expected to observe acceptor-type behavior, but the change in energy of the first absorption band approximately follows the third ionization potential (after crystal-field corrections) through the series from V^{++} to Co^{++}. The results show that the impurity atom is acting as a donor rather than as an acceptor. We have concluded that in fact the excited orbital is similar to an atomic $4s$ orbital.

II. MATERIALS AND EXPERIMENTAL METHODS

A major part of our research effort was expended in proving to our satisfaction that the absorption spectra of the crystal samples used referred to a particular transition-metal impurity in a particular oxidation state and no other. Crystals were obtained from many sources and their spectra compared; the EPR and visible absorption spectra were examined; and many of the samples were subjected to chemical analysis. An account of these efforts for each impurity ion will be given in Sec. III.

The absorption bands found were unexpectedly weak compared to charge-transfer bands, so the samples used had impurity concentrations of about 0.1 mole %, and thicknesses of 0.4–4 mm. The crystal slabs were given a high polish with a diamond-polishing compound.

Three host materials were used: $KMgF_3$, MgF_2, and CaF_2. The absorption spectrum of the pure host material $KMgF_3$ in a 0.85-mm path length is shown in Fig. 1. This crystal was grown at the Clarendon Laboratory of Physics, Oxford, under the supervision of Hukin. The transmission to 80 000 cm^{-1} was found to be adequate to observe the absorption bands of all the divalent ions from V^{++} to Ni^{++}. The $KMgF_3$ crystal has the cubic

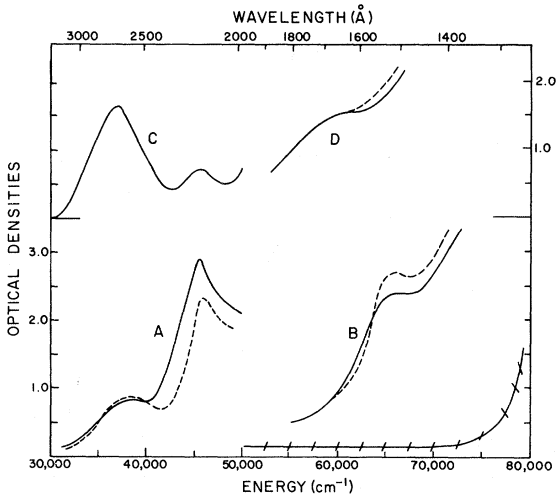

FIG. 1. Hatched line—room-temperature baseline obtained from spectrum of undoped $KMgF_3$ (Hukin), 0.85 mm thick. (a) Near-ultraviolet spectrum of $KMgF_3$:V (Hukin), 3.13 mm thick; $\epsilon = 17.5 \times$ o.d., solid line—room temperature, dashed line—77 °K; (b) vacuum-ultraviolet spectrum of $KMgF_3$:V (Guggenheim), 0.43 mm thick, $\epsilon = 440 \times$ o.d., solid line—room temperature, dashed line—4.2 °K; (c) room temperature near-ultraviolet spectrum of $KMgF_3$:Cr, 9.02 mm thick, $\epsilon = 12.9 \times$ o.d. for those features due to Cr^{++}; (d) vacuum—ultraviolet spectrum of $KMgF_3$:Cr, 0.89 mm thick, $\epsilon = 130 \times$ o.d; solid line—room temperature, dashed line—4.2 °K.

perovskite structure and the impurity, replacing a Mg^{++} ion, is in an octahedral site, with six F^- ion neighbors. In MgF_2 the coordination is octahedral with a small orthorhombic distortion. We hoped that this distortion would split degenerate states as would be revealed by polarization studies. In CaF_2 the coordination is eightfold cubic. The transmission of 1-mm layers of MgF_2 and CaF_2 is high until about 1200 Å.

The absorption spectra were taken with a McPherson 2-m vacuum grating spectrograph Model 2162. Using a 1200-line/mm grating the plate factor is 4.16 Å/mm, and the resolving power using 10-μ slits is 0.08 Å. It was found that none of the spectra had any fine structure and the high resolving power was unnecessary. Therefore most of our results are reported at 1-Å resolution.

The light sources used were microwave powered xenon and krypton lamps. Our early work was done using photographic detection, but for all of the results reported here a photoelectric detection system was used. The photomultiplier was an EMR Model 541G-08-18, an 18-stage solar blind end-on tube with a LiF window and CsI photocathode. The dark count of this tube when operating at 2300 V was less than 0.2/sec.

The detection system was a quantum counting arrangement consisting of an amplifier-discriminator and rate meter.

The sample was mounted at the source end of the spectrograph. It was shown that no photochemical changes occurred as a result of irradiation by the source. A MgF_2 Rochon polarizer was mounted after the sample when studying oriented anisotropic samples. The sample could be mounted on a Cryo-Tip Liquid Transfer Refrigerator (Air Products Co.) by means of which the temperature could be varied from 4 to 300 °K.

The optical density of the sample was determined as follows. The light intensity transmitted through the system as a function of wavelength was determined both with and without the sample in the sample holder, and the data were digitized and stored on paper tape. They were then processed by a H. P. 2116 A computer to give optical density. There was a constant background optical density in most of the absorption curves nearly independent of wavelength; it did not affect the band shape, and was subtracted when taking band area. The background level could be compared with readings of a Cary 14 spectrophotometer in the 1900–2000-Å region and these usually agreed quite well.

The optical density data for a given crystal obtained with several different sources and detectors, agreed within experimental error. For example, some of our early work using a Garton flash lamp and photographic detection gave essentially the same results as the photon counting system used later.

Ultraviolet irradiations were performed with a quartz mercury pen lamp to bleach F centers or other bands.

Chemical analyses were performed by Schwarzkopf Microanalytical Laboratory, Woodside, N. Y.

III. RESULTS

A. $KMgF_3$ host crystal

(1) V^{++}. Two samples of $KMgF_3 : V^{++}$ were studied, one grown by Guggenheim (HG) and loaned to us by Sturge, both of Bell Laboratories, and the other grown by Hukin (DH) of the Clarendon Laboratory, Oxford. Both samples showed the well-known d-d bands of[15] V^{++} and in addition broad bands at 2640 Å (38 000 cm^{-1}), 2150 Å (45 500 cm^{-1}) and 1530 Å (65 400 cm^{-1}). No trace of the strong V^{+++} band at 15 000 cm^{-1} was observed[16] in either sample. The EPR spectrum of the Guggenheim sample showed only the V^{++} signal at 77 °K, and the Hukin sample showed in addition a very weak signal at high g. Optically, the Hukin sample had a more rapidly rising cutoff at 70 000 cm^{-1} than the Guggenheim sample. Based on the d-d and EPR spectra these samples had concentrations of 0.2-mole % V^{++} (HG) and 0.69-mole % V^{++} (DH).

Figure 1(A) shows the near-uv bands of the DH

sample at 77 and 300 °K in a 3.13-mm sample, and Fig. 1(B) shows the high-energy band of the HG sample at 4 and 300 °K in a 0.43-mm thickness. These bands are not affected by heating or uv irradiation. The conversion to molar extinction coefficient ϵ is given in each figure caption in this paper.

The definition of ϵ is $\epsilon = \rho/cl$, where the optical density $\rho = \log(I_0/I)$, c is the concentration in moles/liter, and l is the path length in cm. The oscillator strength calculated from the area under the absorption band is obtained from the equation

$$f = 4.32\times10^{-9}\int \epsilon\, d\bar{\nu}(\bar{\nu} = \nu/c) \ .$$

The energies and f values of the bands are given in Table I at the end of this section.

(2) Cr^{++}. A crystal of $KMgF_3$: Cr was grown for us by Hukin. A chemical analysis found chromium at a level of 0.32 mole %, iron at 0.058 mole %, and no traces of vanadium, manganese, or nickel. However, the dominant feature in the EPR is the divalent manganese spectrum which has been previously identified.[17] The detailed structure observed indicates a low concentration of this species. At $g = 1.977$ there is also a signal due to cubic Cr^{+++} which has its greatest intensity for $\vec{H} \parallel \langle 100 \rangle$. As θ, the angle between the field and the $\langle 100 \rangle$ axis increases the Cr^{+++} signal diminishes in intensity and becomes hidden in the Mn^{++} spectrum for θ greater than 25°. At approximately three orders of magnitude weaker there is a series of over a dozen resonances presumably due to noncubic Cr^{+++}. These are highly orientation dependent and can be eliminated by a heating of the crystal at 600 °C for less than a minute.

The visible d-d bands of Cr^{++} expected at 15 000 cm^{-1} could not be observed in this sample, but bands at 2750 Å (36 400 cm^{-1}), 2180 Å (46 000 cm^{-1}), and 1700 Å (59 000 cm^{-1}) were found. The near-uv bands are shown in Fig. 1(c) at room temperature, and the vacuum uv band is shown in Fig. 1(d) at room temperature and 4.2 °K. Neither the iron nor manganese impurities contribute to these bands (see subsections 3 and 4). However, the F center in $KMgF_3$ appears in the region of the 2750-Å band. Indeed it was found that uv irradiation decreased the intensity of this band by 15%, not completely bleaching it as in the case of F centers in the pure material. However, two hours of heating at 650 °C completely eliminated the band. Therefore, the 2750 Å band is attributed to color centers in the material, perhaps F centers associated with trivalent chromium. The other two bands are not affected by either the irradiation or by the heat treatment. The data on these two bands are listed in Table I.

(3) Mn^{++}: Three samples of $KMgF_3$: Mn were compared: (a) from Sturge and grown by Guggenheim, (b) grown by Hukin, and (c) from Sibley. All samples had the same optical spectrum. No d-d bands were found or were expected to be found in thin layers of this material, and the spectrum is blank until 1660 Å (60 200 cm^{-1}), where a single band is observed. Sample (a) had 3% Mn according to Sturge.[18] Its EPR spectrum at 77 °K showed Mn^{++} and no other signals.

The high-energy spectrum is shown in Fig. 2 at two temperatures for the Guggenheim sample. Although the crystal is only 0.46 mm thick, there is a strong rise at 70 000 cm^{-1} which was obtained reproducibly, and it probably represents another Mn^{++} transition. Note that as with the 45 500 cm^{-1} V^{++} band [Fig. 1(a)] the band strength in Fig. 2 decreases strongly with decreasing temperature.

(4) Fe^{++}: A total of seven bands, none of them Fe d-d transitions, is seen in various combinations in the five iron doped samples which were studied. The bands appear at I 3000–3100 Å (30 000 cm^{-1}), II 2800 Å (35 700 cm^{-1}), III 2200 Å (45 400 cm^{-1}), IV 2040 Å (49 000 cm^{-1}), V 1760 Å (56 800 cm^{-1}), VI 1560 Å (64 000 cm^{-1}), and VII 1470 Å (68 000 cm^{-1}). Three of the samples were purchased from Optovac, Inc., and are denoted Fe Optovac (displaying bands III–VII); Fe(A), which contains 0.082-mole % Fe and 0.0029-mole % Ni (bands III–VII); and Fe(B), which contains 0.084-

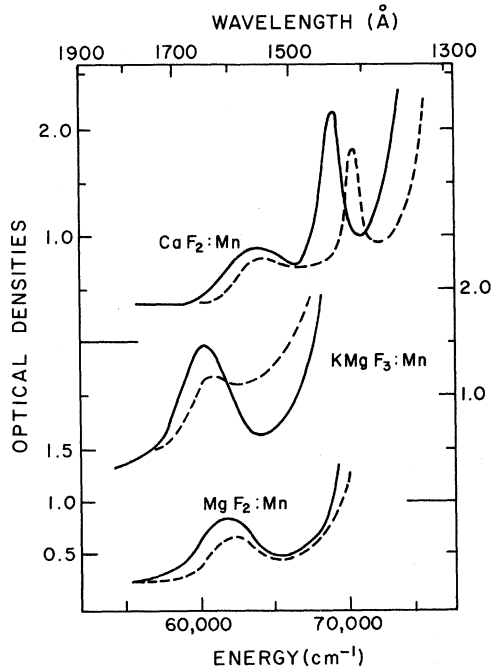

FIG. 2. Vacuum-ultraviolet spectra of Mn^{++} in different host crystals; solid lines—room temperature dashed lines—4.2 °K; $KMgF_3$:Mn (Guggenheim), 0.46 mm thick, $\epsilon = 27.3\times$ o.d.; MgF_2:Mn, 0.71 mm thick, $\epsilon = 110\times$ o.d.; CaF_2:Mn, 1.01 mm thick, containing both Mn^{++} and Fe^{++} $\epsilon = 260\times$ o.d. for Mn^{++} and $870\times$ o.d. for Fe^{++}.

mole % Fe and less than 0.02-mole % Ni (bands IV, VI, and VII). A sample grown by Hukin contains 0.082-mole % Fe and 0.013-mole % Ni (bands I, II, IV, VI, and VII). The fifth sample, grown by Guggenheim, was doped with nickel but contained more iron—0.28-mole % Fe as opposed to 0.041-mole % Ni (bands IV, V, and VII).

All of the samples show band IV which is not seen in the samples containing only nickel (subsection 6). Therefore, it is not a nickel transition, and the self-consistency of the oscillator strengths of this band from crystal to crystal indicate that it is an Fe^{++} transition. Thus this band can be used as a check on the others by noting their intensities relative to it. Its properties are given in Table I.

The near-uv spectra of the Hukin sample are the upper curves shown in Fig. 3(d). The Hukin sample was the only one to display bands I and II, which overlap at room temperature and are only partially resolved at 77 °K, and was the only colored sample, magenta. uv irradiation for a few minutes or heating at 600 °C for 1 min bleached the color and band II. Therefore band II is identified as the $KMgF_3$ F center.[19,20] Band I is then more clearly seen. Its absorption has no temperature dependence and it cannot be bleached with prolonged heating or irradiation. Although the nature of this band is not known, it is seen in some of the $KMgF_3$ samples doped with other metals and therefore cannot be assigned to any ion. In particular, it is not an Fe absorption as none of the other four Fe doped crystals show it. Nor does it correspond to any features in the EPR, which for the Hukin crystal are Mn^{++} resonances, the tetragonal Fe^{+++} center,[21] and the Fe^{++} signal which appears only at liquid helium temperatures.[22]

The Optovac and Fe(A) samples give the same results. The near uv of the Optovac sample is shown in Fig. 3(b). Band III becomes resolved at helium temperatures but since it is seen only in these two samples, it will not be assigned to Fe. The EPR shows the Mn^{++} spectrum and shows Fe^{++} at liquid helium temperatures.

The Guggenheim sample shows the nickel $^3T_{1g}(P)$ d-d band at liquid helium temperatures. Only band III appears in the near uv. The EPR shows Ni^{++}

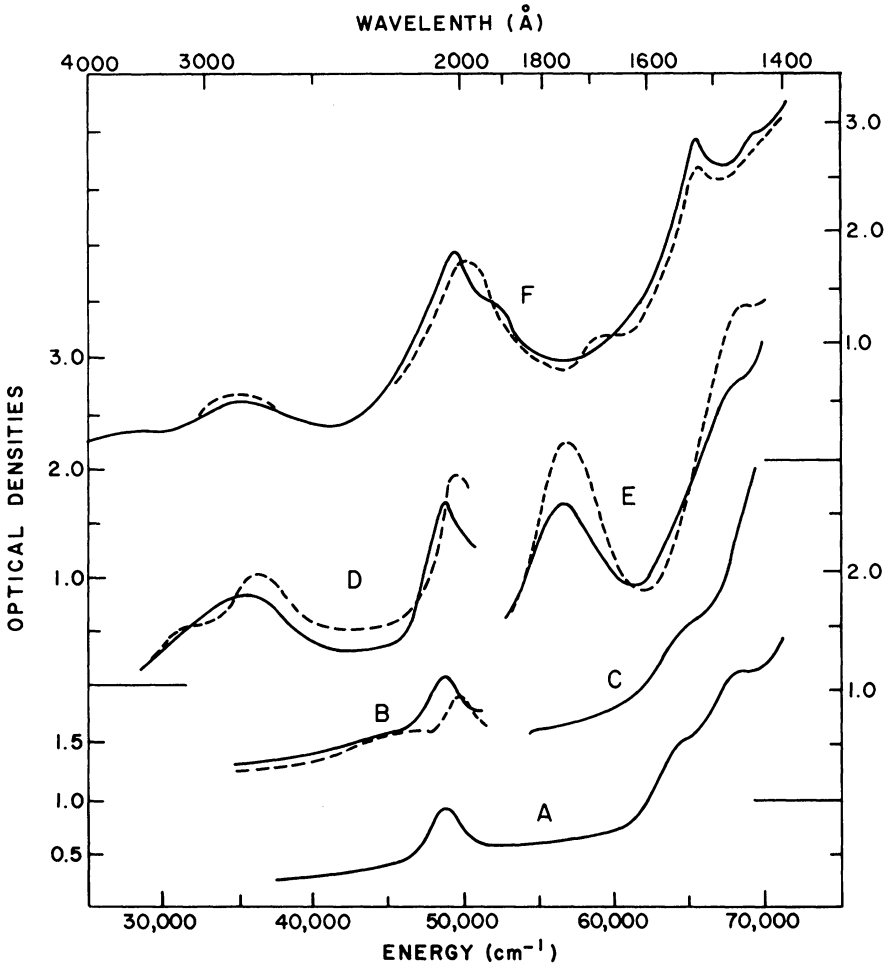

FIG. 3. Ultraviolet spectra of crystals containing Fe^{++} and/or Ni^{++}; solid lines—room temperature dashed lines—4.2 °K, except as noted. (a) $KMgF_3$:Fe (B), 3.51 mm thick, $\epsilon = 128 \times$ o.d.; (b) $KMgF_3$:Fe (Optovac), 5.63 mm thick, $\epsilon = 82 \times$ o.d. for those features due to Fe^{++}; (c) $KMgF_3$:Ni (Dietz), 0.97 mm thick, $\epsilon = 28 \times$ o.d. for any features due to Ni^{++}; (d) $KMgF_3$:Fe (Hukin), 12.78 mm thick; $\epsilon = 36 \times$ o.d. for those features due to Fe^{++}, dashed line—77 °K; (e) $KMgF_3$:Ni (Guggenheim), 0.89 mm thick, containing both Ni^{++} and Fe^{++}; (f) MgF_2:Fe, 0.57 mm thick; $\epsilon = 56 \times$ o.d.

resonances and the Mn^{++} spectrum. In addition, some weak peaks are seen at higher g values, and the Fe^{++} spectrum is seen at helium temperatures.

The Fe(B) sample is perhaps the best iron-doped sample we have. Only the Mn^{++} EPR is seen at room temperature and the Fe^{++} at helium temperatures. In addition, this sample gives the cleanest near-uv and vacuum-uv spectra which are shown in Fig. 3(a).

In the vacuum uv, the Guggenheim sample is the only one to show a clearly defined peak V [see Fig. 3(e)]. This peak is about three times as intense as peak IV in the same sample. Yet in the Fe(B) sample in which peak IV has an o.d. of 0.80, there is no trace of peak V. Therefore, peak V cannot be assigned as an Fe^{++} transition. All of the samples show vacuum-uv peaks VI and VII, but it is not clear as to whether these are Fe transitions or Ni transitions, or neither. The band characteristics according to the first two possibilities are given in Table I.

(5) Co^{++}: Several crystals of $KMgF_3$ doped with Co were obtained from Hukin, and one sample grown by Guggenheim was obtained from Sturge. The Co^{++} resonance at $g = 4.37$ is clearly seen in the EPR at 77 °K in the Guggenheim sample.[23] This sample also shows the Co^{++} d-d absorption bands from which a Co^{++} concentration of 1.5 mole % is estimated.[24] The only higher-energy band in this sample, at 1600 Å (62 600 cm^{-1}) decreases in integrated intensity and shifts to higher energy upon cooling the crystal (Fig. 4). There is a suggestion of another weak band at the edge of the high-energy cutoff. It becomes more prominent at low temperatures. The relatively low-energy cutoff is probably due to a third transition, but the high Co concentration prevents thinning the sample enough to observe another band. It contributes absorption in the region of the 1600-Å band and at low temperatures may produce the long wavelength tail of the band.

(6) Ni^{++}: In addition to the iron-doped samples which contain nickel as an impurity, several nickel-doped samples were studied. The first was given to us by Dietz, of Bell Laboratories and on the basis of the d-d transitions contains 1.4-mole % Ni^{++}.[25,26] The other samples were given to us by Hukin and contain 1.2–5.5-mole % Ni^{++}. All of the samples showed EPR characteristic of a Ni^{++} $^3A_2$ ground state—a $\Delta m = 1$ peak at $g = 2.3$ and a forbidden $\Delta m = 2$ peak at $g = 4.6$, which is about 10% as intense. In addition, the Hukin samples showed a variety of other resonances. The vacuum-uv spectrum of the Dietz sample is shown in Fig. 3(c). The band seen is the same as band VI in the iron-doped samples. All of the Hukin samples show a cutoff around 60 000 cm^{-1}.

The assignment of bands VI and VII in the iron-doped samples to the proper ion is difficult. Because of the strongly increasing background, the intensity to ascribe to these bands cannot be known with any accuracy. This is the only case in which the problem was encountered, as these are the highest-energy bands observed in any of the crystals. If they are nickel transitions, then their intensities in the iron-doped samples indicate oscillator strengths much higher than those of any of the other bands seen for any ion in $KMgF_3$. This would explain the early cutoffs in the rather heavily doped nickel Hukin samples. On the other hand, the Ni (Dietz) sample gives a much lower calculated oscillator strength for band VI. If the band VI is due to iron then its nonappearance in the iron-containing Ni (Guggenheim) sample is puzzling.

B. MgF_2 host crystal

(1) Mn^{++}. A sample of MgF_2 containing 0.26-mole % manganese was obtained from Dietz. None of the spin-forbidden d-d bands can be seen, but a vacuum-uv band at 1620 Å (61 600 cm^{-1}) appears and is shown in Fig. 2. The band decreases in in-

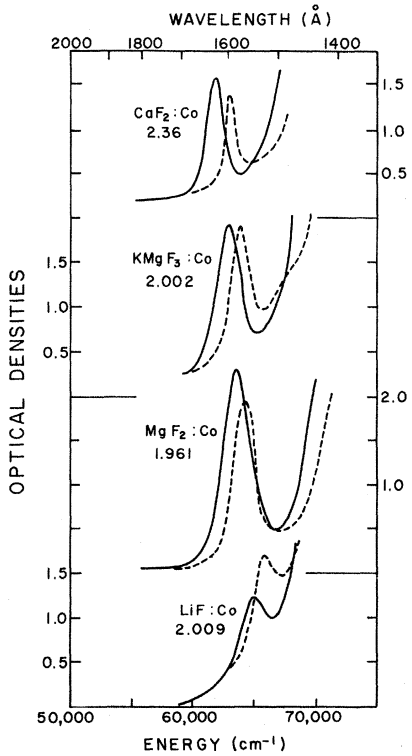

FIG. 4. Vacuum-ultraviolet spectra of Co^{++} in different host crystals with crystal metal-fluorine distances in Å indicated, solid lines—room temperature, dashed lines—4.2 °K, $KMgF_3$:Co (Guggenheim), 0.80 mm thick, $\epsilon = 31 \times$ o.d.; MgF_2:Co (Sibley), 0.68 mm thick, $\epsilon = 15 \times$ o.d.; CaF_2:Co, 0.77 mm thick, $\epsilon = 320 \times$ o.d.; LiF:Co, 4.90 mm thick, $\epsilon = 100 \times$ o.d.

tensity and moves to higher energy with decreasing temperature. As is true for all the bands observed in MgF_2, no polarization was found although the ion has D_{2h} site symmetry.

(2) Fe^{++}. A crystal of MgF_2: Fe was kindly given to us by Dietz. Chemical analysis showed 0.62-mole % Fe and less than 0.01-weight % nickel and vanadium. No d-d transitions were seen, but there are several peaks at higher energy which are shown in Fig. 3(f). Transitions which seem to correspond to bands IV, VI, and VII of the $KMgF_3$: Fe systems are seen. As in $KMgF_3$, there are numerous peaks whose identity is difficult to establish.

(3) Co^{++}. Two crystals of cobalt doped into the MgF_2 lattice were studied. One was given to us by Dietz and the other by Sibley. The samples show identical spectra. The spectrum of the Sibley sample, which contains 2-mole % Co^{++}, is shown in Fig. 4. Again the intensity decrease and energy shift at lowered temperatures and the sharp rise before 70 000 cm^{-1} should be noted.

C. CaF_2 host crystal

This material is both indiscriminate and voracious as a solvent for metal ions. Of approximately 20 transition-metal-doped samples which were obtained, only two were of high enough purity to present in this work.

(1) Mn^{++}: We purchased a sample of CaF_2: Mn from Optovac which gave an EPR spectrum quite similar to those previously published.[27] Chemical analysis showed 0.092-mole % manganese and 0.028-mole % iron. Although no d-d transitions of either ion are observed, vacuum-uv peaks are seen at 1560 Å (64 300 cm^{-1}) and 1440 Å (69 400 cm^{-1}) and are shown in Fig. 2.

This crystal, one of seven doped CaF_2 crystals purchased from Optovac was the only one that transmitted in the vacuum uv and gave rise to distinct absorption bands. It was subjected to destructive testing in analyzing for the iron and manganese content, and it is not known which other transition-metal ions, if any, are present. Since our experience with Optovac grown calcium fluoride crystals indicates possible contamination, we cannot with any degree of confidence assign either of the two vacuum-uv bands.

(2) Co^{++}: We received a pink crystal of CaF_2: Co from Weakliem of the RCA Sarnoff Center, Princeton. The cobalt concentration of the bulk of this sample was much too high for our use; however, a rather large concentration gradient existed. From the most weakly doped portion, we were able to cleave a thin slice that showed both the most intense d-d bands and a vacuum-uv band. The high-energy transition is shown in Fig. 4.

Chemical analysis of a piece of this crystal showed a cobalt concentration of 0.10 mole %. The data on this band are given in Table 1.

D. Band intensities

The bands observed and assigned are listed in Table I. The position and f number is given for each band at 300 and 77 or 4 °K.

Figure 5 shows the temperature dependence of the oscillator strength of the 1600 Å band in $KMgF_3$: Co. From slopes of lines drawn through the data points, values ranging from 130 to 280 cm^{-1} can be obtained for $h\nu$ in the expression $f(T) \cong f(4.2°) \times \coth^{-1}(h\nu/2kT)$. The difficulty in fitting the data is a result of the underlying intensity discussed earlier. Nonetheless, the band is vibronically induced, a result consistent with the low f numbers of all the bands and with their change of intensity from 300 to 4.2 °K given in Table I.

IV. DISCUSSION

There are two classes of transitions which can be thought of that would give rise to the observed high-energy absorption bands. The first of these is the ligand-to-metal charge transfer in which the transition-metal ion acts as an acceptor for an electron which originates on the fluoride ion. In the second class the electron transfer is in the reverse direction, away from the transition ion. Here the ion acts as an electron donor either to the conduction band or to higher localized states of the impurity ion.

Our original expectation was that we would observe bands of the acceptor type, as was seen in the Tippins and Schatz studies. In terms of a local cluster model, transitions from the t_{1u} or t_{2u} ligand molecular orbitals to the metal d shell are parity allowed and give rise to absorptions with oscillator strengths on the order of 10^{-2}. However, the bands

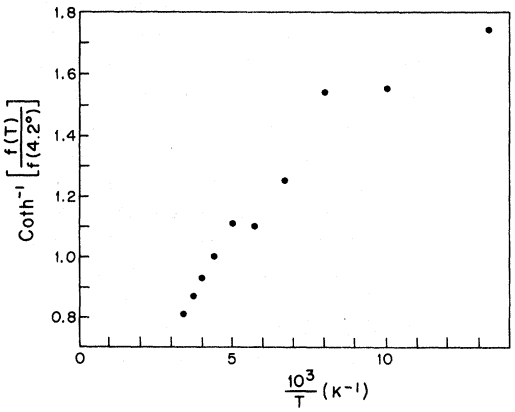

FIG. 5. Temperature dependence of the oscillator strength of the vacuum-ultraviolet band in $KMgF_3$:Co. The tail on the low-energy side of the band is included in the baseline which is assumed to extend to the minimum near 65 000 cm^{-1} where it merges with the cutoff.

TABLE I. Absorption bands of the transition-metal ions in fluoride host crystals in the range from 5 to 10 eV.

System	Temperature (°K)	Position of band maxima (cm^{-1})	Full width at half-maximum (cm^{-1})	Extinction coefficient (liters/mole-cm)	Oscillator strength
$KMgF_3$:V	300	38 000	7 000	13	3.9×10^{-4}
	77	38 000	7 000	14	4.1×10^{-4}
	300	45 500	5 000	49	1.1×10^{-3}
	77	45 800	3 500	39	5.9×10^{-4}
	300	65 400	7 000	770	2.3×10^{-2}
	4.2	65 800	6 000	1100	2.8×10^{-2}
$KMgF_3$:Cr	300	46 400	5 000	9.2	2.0×10^{-4}
	300	59 000	9 000 (?)	130	5.0×10^{-3}
	4.2	59 000	10 000 (?)	156	6.8×10^{-3}
$KMgF_3$:Mn	300	60 200	3 500	25	3.7×10^{-4}
	4.2	60 600	2 500	18	1.9×10^{-4}
$KMgF_3$:Fe	300	49 000	4 400	40	7.5×10^{-4}
	4.2	49 000	4 400	40	7.5×10^{-4}
			4 500	112[a]	2.3×10^{-3}
	300	64 000	4 500	3400[b]	6.5×10^{-2}
				160[a] (?)	2.6×10^{-3}
	300	68 000	3 500	4900[b] (?)	7.3×10^{-2}
$KMgF_3$:Co	300	62 600	2 000	40	3.5×10^{-4}
	4.2	63 500	1 700	40	2.9×10^{-4}
$KMgF_3$:Ni	300	64 000	6 000 (?)	28	7.3×10^{-4}
MgF_2:Mn	300	61 600	4 200	61	1.1×10^{-3}
	4.2	62 500	4 500	45	8.8×10^{-4}
MgF_2:Co	300	63 300	3 000	35	4.5×10^{-4}
	4.2	64 200	2 000	28	2.5×10^{-4}
CaF_2:Co	300	61 500	1 900	450	3.7×10^{-3}
	4.2	62 700	1 300	380	2.1×10^{-3}

[a]Assuming band to be an Fe transition.

[b]Assuming band to be a Ni transition.

we have observed are much weaker than this (see Table I). In addition, because of the temperature dependences of the observed oscillator strength, we conclude that we are dealing with Laporte forbidden transitions in many of the bands. It could be argued that we are seeing transitions from the highest ligand orbital, the t_{1g}. However, from an examination of previous charge-transfer data, we would expect to see the next transition, which would be allowed, at several thousand cm^{-1} to higher energy. This does not fit in with the energy differences of the lowest-energy band and the possible tail of an allowed band over 30 000 cm^{-1} higher in vanadium and chromium or 20 000 cm^{-1} in iron. Also, the band shift to higher energy upon cooling the crystal is not predicted for a charge-transfer acceptor transition, and none has been seen in the previous studies.

The most convincing argument that the transitions we see are not metal acceptors is based on the trends in band positions as we proceed across the Periodic Table from one ion to the next. Following the approach used by Tippins we find that the energy of a transition should be

$$h\nu = C - I_2 + \Delta E_d \ , \tag{1}$$

where C is a constant independent of metal and includes effects such as the Madelung energy and the binding energy of the electron and the hole it leaves behind on the fluorides. I_2 is the electron affinity of the metal ion, and $\Delta E_d = \delta E^{+2} - \delta E^{+1}$ the difference in crystal-field stabilization energy between the divalent ion before the charge-transfer transition and the resulting monovalent species after the transition. The important term in determining energy trends is the electron affinity. As we proceed across the periodic table the increase in nuclear charge and the inability of the d electrons to shield it completely means that the electrons become more tightly bound, resulting in smaller ions and an increase in electron affinity. Thus we would expect a general shift to lower energy as we move across the Periodic Table.

The band positions using Eq. (1) are tabulated in Table II. Instead of merely considering whether the electron is transferred to a t_{2g} or e_g metal or-

TABLE II. Calculated band positions for acceptor, donor, and $3d-4s$ transitions compared to observed band positions for divalent ions.[a] All units are $10^3 cm^{-1}$. In the calculations, the same values of crystal-field parameters B and Dq were used for both the initial and final states. V: $D_q=1.215$; $B=0.720$; Cr: $Dq=1.2$; Mn: $Dq=0.780$; Fe: $Dq=0.90$; $B=0.950$; Co: $Dq=0.780$; $B=0.880$; Ni: $Dq=0.725$; $B=0.955$. There are standard values for the divalent ions.

	Acceptor: $C=175.1$			Donor: $C=-206.9$			$3d-4s$: $C=2.4$			
Metal Ion	$-I_2$	ΔE	E^A calc.	I_3	ΔE	E^D calc.	Free atom	ΔE	E^{ds} calc.	E_{obs}
V	−114.6	7.4	67.8	236.5	6.4	35.6	43.9	6.1	52.4	45.5
Cr	−133.1	7.0	49.0	249.7	−7.0	35.8	49.5	−7.0	44.9	46.4
Mn	−111.8	−3.1	(60.2)	271.8	−4.7	(60.2)	62.5	−4.7	(60.2)	60.2
Fe	−128.7	−2.5	43.9	247.2	3.6	43.9	41.0	3.6	47.0	49.0
Co	−137.6	−4.2	33.3	270.2	2.1	65.4	55.7	2.1	60.2	62.6
Ni	−146.4	4.4	33.1	283.7	3.9	80.7	61.3	3.9	67.6	68 (?)
Cu	−163.7	4.8	16.2	297.1	−4.8	85.4	67.0	−4.8		

[a]Refer to text for formulas used to find E(calc) in the three cases. In each case the Mn^{++} band was used to determine the constant C whose value is given in the column headings.

[b]E_{obs} refers to ions in $KMgF_3$ at 300 °K.

bital, we have refined the calculation of ΔE_d to include the spectroscopic terms observed by using the expressions given in Lever.[31] Thus the metal ionization potential represents the energy absorbed in a transition from the ground-state free-ion term in one oxidation state to the ground-state free-ion term in a second oxidation state. ΔE_d corrects this energy value for the difference between the lowest-energy crystal-field level and the center of the configuration involved, both in the initial and final states.

In Fig. 6, we reproduce the absorption spectra and indicate the energy positions from Table II. The absorption band in $KMgF_3$: Mn has been arbitrarily chosen as the zero of energy since the energy differences between bands and not their absolute positions are meaningful. As can easily be seen, the data do not fit the trends predicted by this charge-transfer model. Thus we have a process which is fundamentally different from that described in previous works.

We now consider the possibility that the absorption bands observed are due to donor transitions. There are two schemes we can employ. In the first, the electron is donated to the host-metal s conduction band and the trends follow the ionization potential of the transition ion. Using $h\nu = C + I_3 + \Delta E_d$, where we have corrected for the energies of the terms as before, we get the results shown in Table II. Again the absorption band in $KMgF_3$: Mn has been arbitrarily chosen as the zero of energy.

In the second donor scheme, we consider the transition to be an electron donation from the localized d shell to the delocalized $4s$ orbit of the impurity metal. Therefore $h\nu = E(3d-4s) + \Delta E_d + C$.

For the ions V^{++}, Cr^{++}, and Mn^{++} there are no paired spins in the ground state, and the lowest energy $d^{n-1}s$ state has the same spin multiplicity. The ions Fe^{++}, Co^{++}, and Ni^{++}, on the other hand, have at least one paired spin in the ground state while the lowest $d^{n-1}s$ state has a higher spin mul-

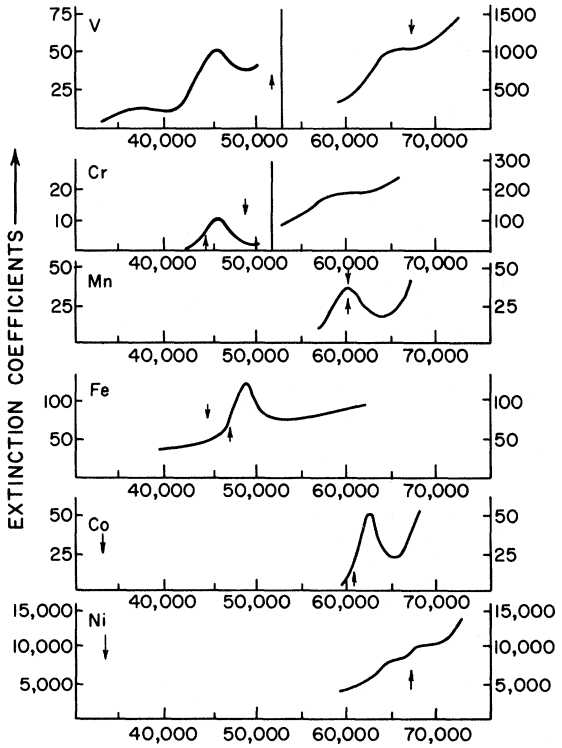

FIG. 6. Comparison of the absorption bands of V^{++} through Ni^{++} in $KMgF_3$. The downward arrows indicate expected positions of acceptor transitions using Mn^{++} to calibrate. The upward arrows show the $3d$-$4s$ positions.

tiplicity. Hence these transitions are $\Delta S = 1$ spin forbidden while the states of the same spin multiplicity as the ground state lie about 10 000 cm^{-1} to higher energy. It is these spin-allowed states to which the data have been fitted.

As can be seen from Fig. 6 and Table II, the donor schemes are much better able to fit the data. It should be realized that the two schemes are not totally different. They both picture the electron as originating on a localized d orbital of the impurity and being donated to an orbital which is more delocalized in the lattice. Although we have given two different zero-order approximations to the final delocalized orbital, in practice it will be somewhere between the two approaches. That is to say, there will be both host-metal s-band character and transition-ion $4s$ orbitals mixed into the final state.

In addition to the trends in the band positions, the donor scheme also fits the other characteristics of the absorption bands. The low oscillator strength could be understood for $3d \rightarrow 4s$ transitions since they are parity forbidden. Transitions to excited orbitals of the conduction band of the host crystal could also be weak because of the small overlap with the localized $3d$ orbital. The oscillator strength is shown to be around 10^{-3} by direct measurement of optical density combined with chemical analysis, and is shown to be induced by vibrations by the temperature dependence of the absorption strength illustrated in Table I and Fig. 5. Thus it is almost surely parity forbidden.

The bandwidth is consistent with either donor or acceptor hypothesis; in each case the oxidation level of the impurity ion changes in the transition and one expects a large change in the configuration coordinates as a result. The occurrence of just one isolated band for several of the ions is in better agreement with the $3d \rightarrow 4s$ interpretation: in that case only a single spin-allowed upper state is expected in a one-electron transition, while in the acceptor interpretation one would expect a set of bands corresponding to various critical points in the density of states of the valence band. In a cluster model of the acceptor transition, there would be two strong and two weak $\pi \rightarrow d$ transitions within a few eV. This is not what we observe.

The $3d \rightarrow 4s$ assignment is also preferred because the absolute value of the transitions in the solid state are almost the same as in the free atom, if the crystal-field corrections are taken into account. (The value of C is only 2400 cm^{-1}.) The same near-equality is observed in the case of the $4f \rightarrow 5d$ transitions in the rare earth ions.[28] In these cases the binding energy of the excited orbital is at most only 20% less than that of the stable orbital.[29] Therefore, it is quite possible that these wave functions are not heavily perturbed in the crystal and would have nearly the same energies as in the free ion. Another example is the $np \rightarrow (n+1)s$ transition in rare gas solids, which occurs close to the position found in the free atom.[30]

In all cases, as Table II shows, the band observed in the solid state is higher by $5\text{–}10 \times 10^3$ cm^{-1} than in the vapor. The blue shift can be understood in terms of the reduced volume available to the $4s$ orbital in the solid state as compared to the vapor, and is the same phenomenon as the blue shift upon lattice contraction.

The $3d \rightarrow 4s$ assignment might also be tested by examining the response of the transition energy to changes in lattice constant. One would expect a blue shift as the lattice constant is reduced because the $4s$ orbital tries to be orthogonal to the surrounding anions, and a decrease in volume available would increase its kinetic energy. In fact a blue shift is observed upon cooling the crystals from 300 to 4 °K, and part of this shift could be caused by thermal contraction.

If the thermal contraction is taken to be 0.3%, we find

$$(\Delta E/E)/(\Delta a/a) = 6$$

for the case of Co^{++} in $KMgF_3$ where $\Delta E = 1100$ cm^{-1} according to Table II. For a particle in a box the above ratio is 2.

We do not get results obviously consistent with the above when the transition energy of the same ion in different host crystals is compared. Fig. 4 shows the spectrum of Co^{++} in CaF_2 (2.36), $KMgF_3$ (2.002), MgF_2 (1.96), and LiF (2.009), where the number in parentheses is the metal-fluorine distance in the host crystal. The transition energy clearly shifts to the blue as the metal-fluorine distance decreases but $(\Delta E/E)/(\Delta a/a) = 0.3$ when comparing $KMgF_3$ and MgF_2, the pair which are the most similar. There is a substantial blue shift from $KMgF_3$ to LiF although the metal-fluorine distances are almost identical. Perhaps these facts are telling us something about the condition of the impurity ion in the crystal. In any case, the increase of band energy upon lattice compression supports the hypothesis of the $3d \rightarrow 4s$ transition.

While it seems quite definite to us that the $3d \rightarrow 4s$ transitions have been identified in this research, there are a number of questions about the spectra reported here which remain unanswered. The bands at 64 000 and 68 000 cm^{-1} in the samples containing Ni and Fe could be assigned to Ni^{++}, but are then a factor of ten too strong for $3d \rightarrow 4s$. It is possible that these are acceptor-type bands because these transitions are expected to occur at the lowest energy near the heavy end of the transition series. We do not know why so many spurious absorption bands appear in the Fe-doped samples, except to

suggest that defects involving several oxidation states might form more easily in this case than in others. The Cr^{++}-containing samples also need further study. We have no definite evidence for the assignment of the higher-energy band in this case, nor for the analogous case of V^{++}. Except for the Fe – Ni question, all the spectra are definitely assignable to a known transition-metal ion, but the presence of associates between one such metal ion and an impurity anion or defect cannot be ruled out in every case. Further work with other host crystals will help to resolve some of these questions and will be reported on at a later time.

ACKNOWLEDGMENTS

We wish to record our thanks to those who have prepared or donated the crystals used in this work: Howard Guggenheim, Robert Dietz, and Michael Sturge of Bell Laboratories, William Sibley of Oklahoma State University, David Hukin of the Clarendon Laboratory, Oxford, and H. Temple and Herbert Weakliem of RCA Laboratories. We also thank D. Bruce Chase of Princeton for the use of the LiF: Co data shown in Fig. 4, and for his considerable help with the experiments.

---

*Work supported by The National Science Foundation and by the Office of Naval Research, under Contract No. 0014-67-A-0151-0012.

[1]H. H. Tippins, Phys. Rev. B 1, 126 (1970).
[2]C. K. Jorgensen, in *Progress in Inorganic Chemistry*, edited by S. J. Lippard (Interscience, New York, 1970), Vol. 12, p. 101.
[3]P. Day, P. J. Diggle, and G. A. Griffiths, J. Chem. Soc. (Dalton Transactions) 1446 (1974).
[4]C. J. Ballhausen and H. B. Gray, *Molecular Orbital Theory* (Benjamin, New York, 1964).
[5]J. R. Dickinson, S. B. Piepho, J. A. Spencer, and P. N. Schatz, J. Chem. Phys. 56, 2668 (1972).
[6]S. B. Piepho, J. R. Dickinson, J. A. Spencer, and P. N. Schatz, J. Chem. Phys. 57, 982 (1972).
[7]S. B. Piepho, J. R. Dickinson, J. A. Spencer, and P. N. Schatz, Mol. Phys. 24, 609 (1972).
[8]W. H. Inskeep, R. W. Schwartz, and N. N. Schatz, Mol. Phys. 25, 805 (1973).
[9]F. A. Modine, Phys. Rev. B 8, 854 (1973).
[10]G. Kuwabara and K. Aoyagi, Jpn. J. Appl. Phys. Supp. 4, 627 (1965).
[11]R. J. Powell and W. E. Spicer, Phys. Rev. B 2, 2182 (1970).
[12]Y. Sakisako, T. Ishii, and T. Sagawa, J. Phys. Soc. Jpn. 36, 1365 (1974).
[13]J. F. Sabatini, Ph.D. thesis (Princeton University, 1973) (unpublished).
[14]A. E. Salwin, Ph.D. thesis (Princeton University, 1974) (unpublished), Chap. 5.
[15]M. D. Sturge, F. R. Merritt, L. F. Johnson, H. J. Guggenheim, and J. P. Van der Ziel, J. Chem. Phys. 54, 405 (1971).
[16]C. J. Ballhausen and F. Winther, Acta Chem. Scand 13, 1729 (1959).
[17]S. Ogawa, J. Phys. Soc. Jpn. 15, 1475 (1960).
[18]M. D. Sturge (private communication).
[19]T. P. P. Hall and A. Leggeat, Solid State Commun. 7, 1657 (1969).
[20]C. R. Riley and W. A. Sibley, Phys. Rev. B 1, 2789 (1970).
[21]D. C. Stjern, R. C. DuVarney, and W. P. Unruh, Phys. Rev. B 10, 1044 (1974).
[22]J. T. Vallin and W. W. Piper, Solid State Commun. 9, 823 (1971).
[23]T. P. Hall, W. Hayes, R. Stevenson, and J. Wilkins, J. Chem. Phys. 39, 35 (1963).
[24]J. Ferguson, D. L. Wood, and K. Knox, J. Chem. Phys. 39, 881 (1963).
[25]J. Ferguson, H. J. Guggenheim, and D. L. Wood, J. Chem. Phys. 40, 822 (1964).
[26]J. Ferguson and H. J. Guggenheim, J. Chem. Phys. 44, 1095 (1966).
[27]J. M. Baker, B. Bleaney, and W. Hayes, Proc. R. Soc. Lond. A 247, 141 (1958).
[28]T. S. Piper, J. P. Brown, and D. S. McClure, J. Chem. Phys. 46, 1353 (1967).
[29]J. Sugar and J. Reader, J. Chem. Phys. 59, 2083 (1973).
[30]G. Baldini and R. S. Knox, Phys. Rev. Lett. 11, 127 (1963).
[31]A. B. P. Lever, Inorganic Electronic Spectroscopy (Elsevier, New York, 1968), page 182.